JACS
JOURNAL OF THE AMERICAN CHEMICAL SOCIETY

Communication

pubs.acs.org/JACS

Milliseconds Make the Difference in the Far-from-Equilibrium Self-Assembly of Supramolecular Chiral Nanostructures

Alessandro Sorrenti,*[,†,∥] Romen Rodriguez-Trujillo,[†] David B. Amabilino,*[,†,‡] and Josep Puigmartí-Luis*[,†,§]

[†]Institut de Ciència de Materials de Barcelona (ICMAB-CSIC), Campus Universitari de Bellaterra, 08193 Cerdanyola del Vallès,Catalonia, Spain

[‡]School of Chemistry, The University of Nottingham, University Park NG7 2RD, United Kingdom

[§]Swiss Federal Laboratories for Materials Science and Technology (EMPA), Lerchenfeldstrasse 5, 9014 St. Gallen, Switzerland

Supporting Information

ABSTRACT: The effect of diffusion-controlled microfluidic conditions in the very initial stages of a far-from-equilibrium self-assembly process on the evolution of aggregate chirality in a multicomponent supramolecular system is shown.

The control of the expression and transfer of chirality at the supramolecular level can emerge in the organization of molecules into chiral space groups (intrinsically chiral packing)[1−3] or sometimes at higher levels of organization, with the emergence of morphologies such as helices or twisted ribbons.[3,4] Even when using homochiral building blocks, the transfer of chirality at the supramolecular level can be intricate, as shown in the case of amphiphilic molecules in water.[3,5−7] The organization of the whole assembly can be triggered by a fine balance of interactions, including hydrophobic ones.[7] Achiral systems can undergo symmetry breaking upon aggregation, i.e., spontaneous resolution into chiral assemblies. An example is the self-assembly in aqueous acid of achiral sulfonated porphyrins to give J-aggregates.[8,9]

Recently, the structure of the J-aggregates of tetrakis(4-sulfonatophenyl)porphyrin (H2TPPS4) has been resolved, demonstrating that they are intrinsically chiral species and may exist as racemic conglomerates, i.e., racemic mixture of enantiomeric assemblies.[10] In this case, the action of even minimal chiral influences, such as chiral contaminants[11,12] or hydrodynamic vortices[13,14] can induce considerable chiral biases (i.e., formation of scalemic vs racemic mixtures of assemblies).[13−16] The self-assembly of meso-(4-sulfonatophenyl)porphyrins is a hierarchical supramolecular polymerization characterized by a critical nucleation step and different thermodynamic and kinetic growth pathways.[12,17−23] It is possible to exploit this complexity in order to control the aggregation as well as the expression of chirality by varying experimental conditions, including different kinds of mixing. As an example, diastereo and enantioselective growth of J-aggregates of amphiphilic porphyrins under laminar flow conditions (magnetic stirring in square section cuvettes) has been reported.[16,24,25] In addition, the formation of porphyrin assemblies with different sizes (from nano- to micro- scale) and morphologies has been recently achieved employing a kinetically controlled self-assembly process inside a microfluidic chip.[26] Indeed, the controlled reaction-diffusion zone enabled by microfluidic approaches has been advantageously used by us and other groups to fine-tune self-assembly and reaction processes inside microfluidic channels.[27,28]

Herein, we studied the interaction under flask and microfluidic mixing of the diacid zwitterionic form of H_2TPPS_4 (**1**), at pH < 3.5, with cetyltrimethylammonium bromide (**2**)[29−31] both in the presence and in the absence of (*S*)-*N*,*N*-dimethyl-*N*-(1-phenylethyl)hexadecan-1-ammonium bromide (**3**) as a chiral inducer (Figure 1a). One of us first studied the heteroaggregates formed by **1** with chiral cationic surfactants, revealing these systems as excellent models for studying the propagation of chirality to complex supramolecular aggregates.[32,33] However, the results presented here are the first clear example showing that the expression of chirality in an evolving (days time scale) tricomponent supramolecular system can be finely influenced by controlling the nucleation events at the very early stages of the assembly, approximately during the first 20 ms.

When aqueous solutions of **1** (40 μM) and **2** (80 μM) were injected, respectively, in the middle inlet channels (b) and (c), while water and 2 mM $HCl_{(aq)}$ were injected, respectively, through the side inlets (a) and (d), the M1 sample was prepared (see Figure 1b). When added, the chiral inducer **3** was injected at different positions with one of the other components (see Figure 1b samples M2−M4). Due to the laminar flow present in the microchannel, the solution streams coflow, and mixing occurs only through pure molecular diffusion in the chip. The flow rate for the four injected solutions was set at 100 μL min^{-1}, i.e., a flow rate ratio (FRR) of 1 was established to avoid both a complete protonation of the porphyrin and clogging of the microfluidic channel. With these settings, the calculated residence time of the injected species within the chip is 18.7 ms. The solutions coming out of the chip were collected via PTFE tubing to 1 cm quartz cuvettes for the spectroscopic investigations.

To test the actual effect of the diffusion-controlled microfluidic condition on the chirality of the formed aggregates, alike experiments were performed in laboratory flask reactors

Received: March 9, 2016
Published: May 20, 2016

DOI: 10.1021/jacs.6b02538
J. Am. Chem. Soc. 2016, 138, 6920−6923

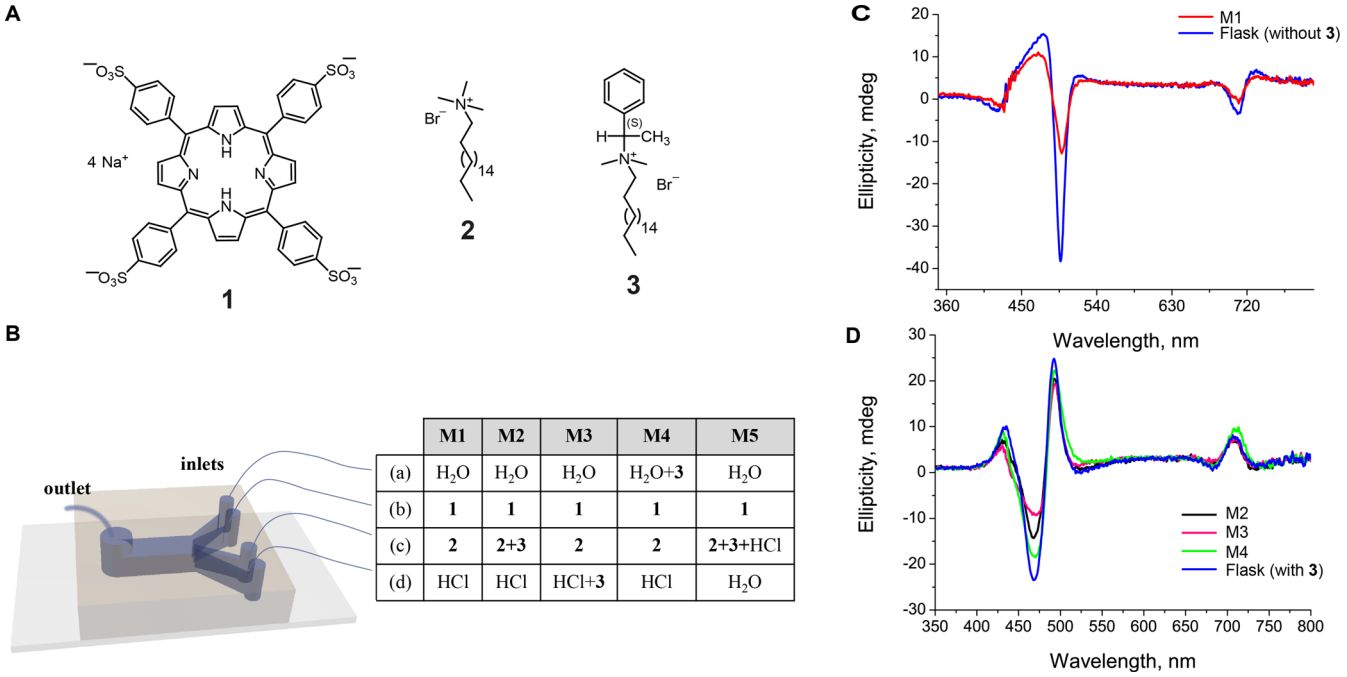

	M1	M2	M3	M4	M5
(a)	H_2O	H_2O	H_2O	H_2O+**3**	H_2O
(b)	**1**	**1**	**1**	**1**	**1**
(c)	**2**	**2**+**3**	**2**	**2**	**2**+**3**+HCl
(d)	HCl	HCl	HCl+**3**	HCl	H_2O

Figure 1. (A) Chemical structures of the investigated compounds. (B) Schematic view of the microfluidic chip used in the experiments together with the configuration used to prepare M1−M5. (C) CD spectra of M1 and flask samples without **3**. (D) CD spectra of M2−M4 and flask samples with **3**.

using standard chaotic mixing protocols (details in SI, Section 1). The same solutions as those injected in microfluidic experiments were used. Both the samples collected from the microfluidic chip and those prepared in flask mixing experiments were stored in quartz cuvettes under identical conditions of light and temperature, and their evolution with time was monitored by UV−vis absorption and circular dichroism (CD) spectroscopy. The typical absorption spectrum of all the investigated samples (whether prepared by microfluidics or flask mixing) shows bands at 434 and 650 nm corresponding, respectively, to the Soret and the main Q-band of the monomeric diprotonated porphyrin **1** (zwitterionic), along with two less intense bands at 495 and 716 nm assigned to J-type surfactant/porphyrin heteroaggregates (see Figure S1).[31] In the absence of **3**, the CD spectra of the flask mixing and M1 samples show the appearance of an asymmetric negative couplet, an excitonic band, in correspondence with the absorption band of the surfactant/porphyrin J-aggregates. Under this condition, a similar behavior is observed for both microfluidic and bulk samples (Figures 1c and S2). The intensity of this dichroic band strongly increases with time, while no relevant changes in the associated UV−vis absorption spectra occur (see Figure S2). Thus, a spontaneous symmetry breaking is observed with the generation of an enantiomeric excess of aggregates whose sign (bias) can be ascribed to the presence of ubiquitous chiral contaminants (e.g., biological debris).[11,12,25] When **3** was added at **2**/**3** ratio 9:1, while keeping constant the total surfactant concentration (at surfactants/**1** ratio of two to 2:1), an opposite CD band (a positive couplet) was observed for the heteroaggregates, both in flask as well as for M2−M4 samples prepared by injecting **3** at different positions inside the microfluidic device (Figure 1d). These results indicate that a chiral surfactant can trigger the desired optical activity of the final surfactant/**1** J-aggregates, hence overcoming the chirality transfer from chiral contaminants during nucleation. Actually, similar competition experiments using compound **3** enantiomers were originally performed in the self-assembly of pure H2TPPS4 (**1**), unequivocally proving the presence of chiral contaminants in ultrapure water.[11] It has to be noted that using our microfluidic approach, in which HCl is injected on a lateral stream ((d) inlet channel), the protonation of the porphyrin can be precisely controlled and/or avoided inside the microfluidic channel, despite the fast proton diffusion due to the Grotthuss mechanism. In particular, finite element simulations of proton diffusion in the microfluidic chip using a computational fluid dynamic software showed that when HCl is injected in (d) inlet channel, the actual pH at the half width of the main channel, and even at the chip output, is well above 4 (see Figure S3); a result that clearly indicates that the protonation of the porphyrin is prevented inside the microfluidic channel. (Refer to Section 3 of SI for further detail about the finite element method used in our simulation studies.)

Optical microscope images acquired during these microfluidic experiments clearly show the formation of purple porphyrin/surfactant heteroaggregates in the microfluidic channel, thus indicating the nonprotonated state of **1** under these conditions (see Figure S5).[31] In the same way, when **3** is disposed in the lateral stream opposite to **1**, in (d) inlet channel (sample M3 in Figure 1b), the chiral inducer **3** cannot encounter the porphyrin within the microfluidic channel length, where mixing only occurs through diffusion. On the other hand, when **3** is pumped in (a), adjacent to **1** (sample M4 in Figure 1b), the formation of neutral **3**/**1** heteroaggregates occurs, as evidenced by the clear boundary between the two stream flows visible in the micrographs of the chip (see Figure S6). These heteroaggregates are probably similar to those previously reported for the **3**/**1** system at neutral pH.[32] To sum up, using these conditions, the encounter between the protonated porphyrin and **2** in the presence of the chiral inducer **3** occurs

DOI: 10.1021/jacs.6b02538
J. Am. Chem. Soc. 2016, 138, 6920−6923

essentially out-of-chip, in the collecting flask and under chaotic mixing, thus giving similar results to bulk samples.

In order to finely control the nucleation and the chiral bias (induction), we decided to inject both surfactants (**2** and **3**) with HCl (aq, 2 mM) in the middle stream, (c) inlet channel, adjacent to the porphyrin stream, (b) inlet channel. This configuration, where M5 samples are produced, ensures a precise control of the protonation of the porphyrin (see Figure S4) as well as a diffusion-based mixing of all the species within the chip, at the early stages of the aggregation process. It should be noted here that in contrast to bulk synthetic approaches, where a specific protonation of the porphyrin at early stages of the self-assembly process is unachievable,[25] controlled microfluidic mixing can circumvent this hurdle. Morover, in our investigations, we reduced the concentration of **3** so to have **2**/**3** ratio 20:1. The formation of a yellow-green deposit on the bottom layer of the chip, where the flow regime is approximately zero due to the no-slip boundary condition, confirms that the protonation of porphyrin occurs in the microfluidic channel as observed in optical micrographs (see Figure S7). Figure 2 shows the CD spectra for the microfluidic and bulk samples recorded soon after the preparation and after 3 days aging together with transmission electron microscopy (TEM) images of both samples. Remarkably, chiral induction by **3** in microfluidic samples showed a positive CD couplet that did not change with time (see Figure 2a,b), while bulk samples evolved with time yielding, after aging, a negative couplet analogous to that observed in the absence of the chiral inducer (compare Figures 2b and 1c). Thus, the effect of difussion-controlled microfluidic mixing at very early stages of nucleation is that of enhancing the chiral selection by the additive, allowing a specific chiral induction event even at lower concentration than in bulk samples. Remarkably, and as shown in Figure 2, a few milliseconds of controlled diffusion mixing under laminar flow conditions are enough to control the expression of supramolecular chirality in the growing heteroaggregates. Similar results were observed also upon decreasing further the concentration of **3** to a **2**/**3** ratio of 20:0.75, confirming the consistency of our observations (Figure S8).

The anisotropic shape of the CD bands and their evolution with time in the case of bulk samples (accompanied by undetectable changes in the corresponding absorption spectra) strongly suggest the presence of different diastereomeric J-aggregates (mesomorphs) absorbing at similar wavelengths and featuring opposite chiroptical features along the hierarchical growth pathway of the **1**/**2** heteroaggregates. This effect is in analogy to that previously reported for homoaggregates of related sulfonated porphyrins.[10,24,25] Thus, a reasonable explanation for the different effect of laminar vs chaotic mixing on the transcription of supramolecular chirality is the formation of different mesomorphs with almost opposite chiroptical features, which would correspond to a different diastereoselection. In addition, the higher intensity of the aggregate's absorption bands at around 500 and 700 nm (see HT profiles in Figure 2) for the bulk sample with respect to the microfluidic one, already observed soon after preparation, suggests differences in the extent of the aggregation (e.g., due to different nucleation rates) and/or in the supramolecular organization of the assemblies (yielding different optical properties). TEM images of the microfluidic and bulk J-type surfactant/porphyrin aggregates are presented in Figure 2c,d, respectively. While disordered assemblies are mainly observed in the bulk samples, well-defined rod-like structures with dimensions of ~500 nm in

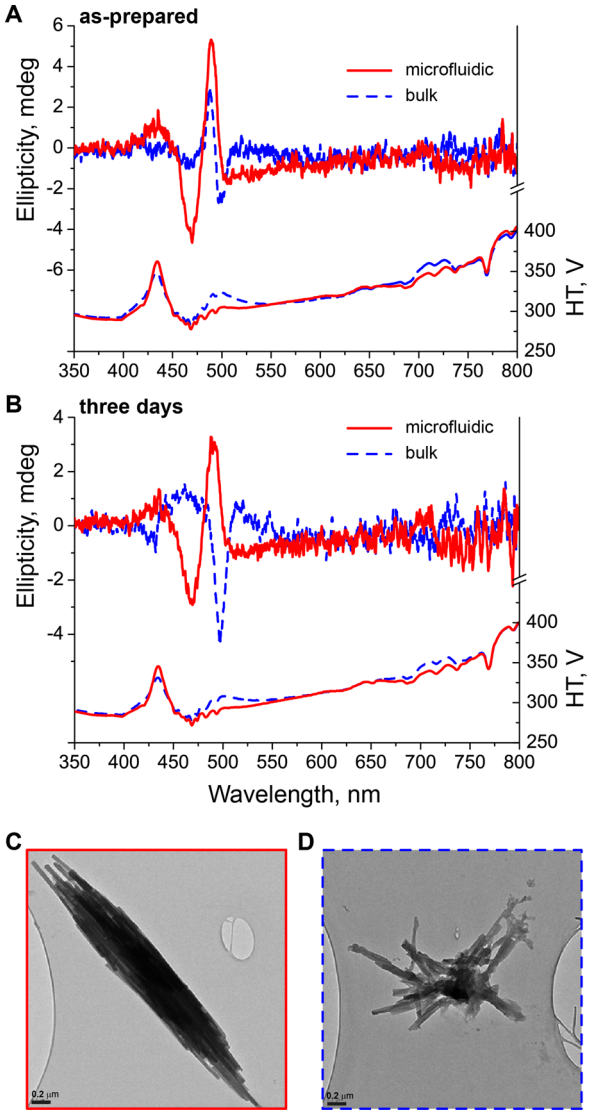

Figure 2. CD spectra and HT voltage profiles for M5 and bulk samples recorded soon after the preparation (A) and after aging for 3 days (B). In (C) and (D), TEM images of heteroaggregates observed in microfluidic and bulk as-prepared samples, respectively.

width and 1 μm in length were found in microfluidic samples, which tend to align along their long axis to form rather ordered clusters. This demonstrates that the morphology of multi-component supramolecular assemblies can also be controlled when aggregation starts under a laminar flow regime.

In conclusion, the work reported here emphasizes the importance of the order of addition and conditions of mixing of the building blocks in self-assembly processes and in the chiral induction. It is important to note that here the chiral selection is reversed over time for bulk samples, while it is maintained for samples prepared under laminar flow conditions. Further, the results reveal how in laminar flow conditions, unique aggregation phenomena can be induced and further observed, thus demonstrating the potential of microfluidic approaches for controling the complex behavior of chirality translation. In contrast to previously reported studies where rotational, magnetic, and gravitational external forces have successfully led to chiral selection in achiral systems undergoing symmetry breaking employing induction times greater than tens of minutes,[13,14] here we make use of rapid and controlled diffusion

DOI: 10.1021/jacs.6b02538
J. Am. Chem. Soc. 2016, 138, 6920−6923

mixing processes (present in microfluidic devices) to modulate chiral induction in the presence of an added homochiral dopant. The microfluidic mixing allows effective influence of nucleation events at the very early stages of the assembly process (during the first tens of milliseconds), resulting in the present case in an opposite evolution of aggregate chirality in the far-from-equilibrium supramolecular aggregates generated, when compared with samples prepared by flask mixing. Hence, we can conclude that very subtle changes in the mixing conditions under diffusion-limited microfluidic environments can also influence the nucleation events, thereby resulting in unexpected chiral selection and symmetry breaking. We believe that this approach paves the way for the investigation of unique aggregation phenomena and chirality translation in multicomponent supramolecular systems.

■ ASSOCIATED CONTENT

Supporting Information

The Supporting Information is available free of charge on the ACS Publications website at DOI: 10.1021/jacs.6b02538.

Information about the microfluidic device together with absorption and CD spectra corresponding to additional experiments of chiral induction under microfluidic conditions and details and discussion of the proton diffusion simulations by COMSOL multiphysics (PDF)

■ AUTHOR INFORMATION

Corresponding Authors

*sorrenti@unistra.fr
*david.amabilino@nottingham.ac.uk
*josep.puigmarti@empa.ch

Present Address

[‖]Institut de Science et d'Ingénierie Supramoléculaires/Université de Strasbourg, 8 allée Gaspard Monge, 67083 Strasbourg (Cedex), France.

Notes

The authors declare no competing financial interest.

■ ACKNOWLEDGMENTS

This work was supported by MINECO (Spain, Project MAT2013-47869-C4). J.P.L. also acknowledges the Ramon y Cajal program (RYC-2011-08071) from the Spanish Ministry of Economy and Competitiveness. D.B.A. thanks the EPSRC. R.R.-T. acknowledges the support from Generalitat de Catalunya and the COFUND programme of the Marie Curie Actions of the 7th R&D Framework Programme of the European Union (BP-B 00256).

■ REFERENCES

(1) Amabilino, D.B., (Ed.), *Chirality at the Nanoscale: Nanoparticles, Surfaces, Materials and More*; Wiley-VCH: Weinheim, 2009.
(2) Crego-Calama, M.; Reinhoudt, D. N. *Supramolecular Chirality. Topics in Current Chemistry*; Springer: Berlin, 2006.
(3) Wang, Y.; Xu, J.; Wang, Y.; Chen, H. *Chem. Soc. Rev.* **2013**, *42*, 2930.
(4) Brizard, A.; Oda, R.; Huc, I. *Top. Curr. Chem.* **2005**, *256*, 167.
(5) Ceccacci, F.; Mancini, G.; Sferrazza, A.; Villani, C. *J. Am. Chem. Soc.* **2005**, *127*, 13762.
(6) Bombelli, C.; Bernardini, C.; Elemento, G.; Mancini, G.; Sorrenti, A.; Villani, C. *J. Am. Chem. Soc.* **2008**, *130*, 2732.
(7) Marinelli, F.; Sorrenti, A.; Corvaglia, V.; Leone, V.; Mancini, G. *Chem. - Eur. J.* **2012**, *18*, 14680.
(8) Ohno, O.; Kaizu, Y.; Kobayashi, H. *J. Chem. Phys.* **1993**, *99*, 4128.
(9) Rubires, R.; Crusats, J.; El-Hachemi, Z.; Jaramillo, T.; López, M.; Valls, E.; Farrera, J.-A.; Ribó, J. M. *New J. Chem.* **1999**, *23*, 189.
(10) El-Hachemi, Z.; Escudero, C.; Acosta-Reyes, F.; Casas, M. T.; Altoe, V.; Aloni, S.; Oncins, G.; Sorrenti, A.; Crusats, J.; Campos, J. L.; Ribó, J. M. *J. Mater. Chem. C* **2013**, *1*, 3337.
(11) El-Hachemi, Z.; Escudero, C.; Arteaga, O.; Canillas, A.; Crusats, J.; Mancini, G.; Purrello, R.; Sorrenti, A.; D'urso, A.; Ribo, J. M. *Chirality* **2009**, *21*, 408.
(12) De Greef, T. F.; Smulders, M. M.; Wolffs, M.; Schenning, A. P.; Sijbesma, R. P.; Meijer, E. W. *Chem. Rev.* **2009**, *109*, 5687.
(13) Ribó, J. M.; Crusats, J.; Sagués, F.; Claret, J.; Rubires, R. *Science* **2001**, *292*, 2063.
(14) Micali, N.; Engelkamp, H.; van Rhee, P. G.; Christianen, P. C. M.; Scolaro, L. M.; Maan, J. C. *Nat. Chem.* **2012**, *4*, 201.
(15) Escudero, C.; Crusats, J.; Díez-Pérez, I.; El-Hachemi, Z.; Ribó, J. M. *Angew. Chem.* **2006**, *118*, 8200.
(16) Ribó, J. M.; El-Hachemi, Z.; Crusats, J. *Atti. Accad. Naz. Lincei* **2013**, *24*, 197.
(17) Pasternack, R. F.; Fleming, C.; Herring, S.; Collings, P. J.; dePaula, J.; DeCastro, G.; Gibbs, E. J. *Biophys. J.* **2000**, *79*, 550.
(18) Monsù Scolaro, L.; Castriciano, M.; Romeo, A.; Mazzaglia, A.; Mallamace, F.; Micali, N. *Phys. A* **2002**, *304*, 158.
(19) Castriciano, M. A.; Romeo, A.; Villari, V.; Micali, N.; Scolaro, L. M. *J. Phys. Chem. B* **2003**, *107*, 8765.
(20) De Napoli, M.; Nardis, S.; Paolesse, R.; Vicente, M. G. H.; Lauceri, R.; Purrello, R. *J. Am. Chem. Soc.* **2004**, *126*, 5934.
(21) Micali, N.; Villari, V.; Castriciano, M. A.; Romeo, A.; Monsù Scolaro, L. *J. Phys. Chem. B* **2006**, *110*, 8289.
(22) Escudero, C.; D'Urso, A.; Lauceri, R.; Bonaccorso, C.; Sciotto, D.; Di Bella, S.; El-Hachemi, Z.; Crusats, J.; Ribó, J. M.; Purrello, R. *J. Porphyrins Phthalocyanines* **2010**, *14*, 708.
(23) Castriciano, M. A.; Romeo, A.; Zagami, R.; Micali, N.; Scolaro, L. M. *Chem. Commun.* **2012**, *48*, 4872.
(24) Sorrenti, A.; El-Hachemi, Z.; Crusats, J.; Ribo, J. M. *Chem. Commun.* **2011**, *47*, 8551.
(25) Sorrenti, A.; El-Hachemi, Z.; Arteaga, O.; Canillas, A.; Crusats, J.; Ribo, J. M. *Chem. - Eur. J.* **2012**, *18*, 8820.
(26) Numata, M.; Kozawa, T. *Chem. - Eur. J.* **2014**, *20*, 6234.
(27) Puigmartí-Luis, J. *Chem. Soc. Rev.* **2014**, *43*, 2253.
(28) Kim, H.; Lee, H.-J.; Kim, D.-P. *Angew. Chem., Int. Ed.* **2015**, *54*, 1877.
(29) Gandini, S. C. M.; Yushmanov, V. E.; Borissevitch, I. E.; Tabak, M. *Langmuir* **1999**, *15*, 6233.
(30) Maiti, N. C.; Mazumdar, S.; Periasamy, N. *J. Porphyrins Phthalocyanines* **1998**, *2*, 369.
(31) Maiti, N. C.; Mazumdar, S.; Periasamy, N. *J. Phys. Chem. B* **1998**, *102*, 1528.
(32) El-Hachemi, Z.; Mancini, G.; Ribó, J. M.; Sorrenti, A. *J. Am. Chem. Soc.* **2008**, *130*, 15176.
(33) El-Hachemi, Z.; Mancini, G.; Ribó, J. M.; Sorrenti, A. *New J. Chem.* **2010**, *34*, 260.

DOI: 10.1021/jacs.6b02538
J. Am. Chem. Soc. 2016, 138, 6920−6923